

# A simplified density functional theory method for charged adsorbates on an ultrathin, insulating film supported by a metal substrate

Iván Scivetti<sup>1</sup> and Mats Persson<sup>1,2</sup>

<sup>1</sup> Surface Science Research Centre and Department of Chemistry, University of Liverpool, Liverpool L69 3BX, UK

<sup>2</sup> Department of Applied Physics, Chalmers University of Technology, SE-412 96 Göteborg, Sweden

E-mail: [scivetti@liverpool.ac.uk](mailto:scivetti@liverpool.ac.uk)

**Abstract.** A simplified density functional theory (DFT) method for charged adsorbates on an ultrathin, insulating film supported by a metal substrate is developed and presented. This new method is based on a previous DFT development that uses a perfect conductor (PC) model to approximate the electrostatic response of the metal substrate, while the film and the adsorbate are both treated fully within DFT [I. Scivetti and M. Persson, *Journal of Physics: Condensed Matter* **25**, 355006 (2013)]. The missing interactions between the metal substrate and the insulating film in the PC approximation are modelled by a simple force field (FF). The parameters of the PC model and the force field are obtained from DFT calculations of the film and the substrate, here shown explicitly for a NaCl bilayer supported by a Cu(100) surface. In order to obtain some of these parameters and the polarisability of the force field, we have to include an external, uniformly charged plane in the DFT calculations, which has required the development of a periodic DFT formalism to include such a charged plane in the presence of a metal substrate. This extension and implementation should be of more general interest and applicable to other challenging problems, for instance, in electrochemistry. As illustrated for the gold atom on the NaCl bilayer supported by a Cu(100) surface, our new DFT-PC-FF method allows us to handle different charge states of adsorbates in a controlled and accurate manner with a considerable reduction of the computational time. In addition, it is now possible to calculate vertical transition and reorganisation energies for charging and discharging of adsorbates that cannot be obtained by current DFT methodologies that include the metal substrate. We find that the computed vertical transition energy for charging of the gold adatom is in good agreement with experiments.

PACS numbers: 68.37.Ef, 73.20.Mf, 73.22.-f

## 1. Introduction

A new frontier in atomic-scale science has opened up by the recent progress in the study by scanning tunnelling microscopy (STM), non-contact atomic force microscopy (nc-AFM) and Kelvin probe force microscopy (KPFM) of single adsorbates on ultrathin-insulating films supported by a metal substrate [1, 2, 3, 4, 5, 6]. Most interesting and unique properties of such films are the near decoupling of the electronic states of the adsorbate with the electronic states of the metal substrate [1] and the ability to stabilise various charge states of adsorbates on polar films, which can be switched in a controlled manner by attachment of tunnelling electrons and holes. These properties have been demonstrated and exploited in many experiments including imaging of frontier orbitals [1, 2], charge state control of adsorbed species [3, 4], coherent electron-nuclear coupling in molecular wires [7] and tunnelling-induced switching of adsorbed molecules [5, 8].

Alongside with the on-going, exciting developments of scanning probe microscopy experiments on these systems, density functional theory (DFT) calculations of their electronic and geometric structure play a crucial role in helping to unravel their physical and chemical properties [3, 4, 5]. Nevertheless, DFT calculations for these systems are very challenging due to their system size, especially, the large number of metal electrons, and the intrinsic self-interaction errors in current exchange-correlation functionals

[9]. The self-interaction error and the associated delocalisation error often result in unphysical, fractional charging of adsorbates. This limitation not only complicates the correct identification of the various charge states, but also leads to failures in the description of the charge transfer process between the metal substrate and the adsorbate. Some possible routes to surmount this limitation is offered by DFT+U [14, 15] or constrained DFT [10]. The DFT+U approach has been applied to adatoms on insulating films [4] but it is not straightforward to extend this approach to molecular adsorbates with delocalised frontier orbitals. Constrained DFT has not so far been applied to this problem. Regardless, all these approaches are very challenging since they still involve a large number of metal electrons. Replacing the metal substrate by a positive homogeneous background was attempted in the calculation of charged adatoms on an ultra-thin insulating film [16].

In this paper we propose a new simplified and approximate DFT method that circumvents these limitations for an adsorbate on an ultrathin insulating film supported by a metal substrate. Here we simply assume that the role of the metal substrate is to set the chemical potential for the electrons, to screen the charge of adsorbates (so that the total system is neutral), and to constrain the motion of the neighbouring atoms in the film to the metals substrate atoms. The proposed method is based on these assumptions and builds on our recently developed DFT scheme [11], where the insulating film and adsorbate are treated fully within DFT and their interaction with the metal substrate is assumed to be purely electrostatic, while the density response of the metal surface to this interaction is treated to linear order. Here, the metal response will simply be approximated by a classical perfect conductor (PC) model, in which the screening charge only resides on the image plane[11]. The residual interactions that are not captured by the PC approximation will be included in a force field (FF) between the insulating film and the metal substrate, whose parameters are determined from DFT calculations for the insulating film and metal substrate in absence of the adsorbate. In the development of this force field it was required to derive appropriate corrections to the DFT formalism (and also for the DFT-PC method) to include an external, uniformly charged layer. Henceforth we will refer to DFT-PC when we compute the DFT problem using the PC model and to DFT-PC-FF when using both the PC model and the force field.

With the DFT-PC-PP method the charge states of adsorbates can now be controlled and the problem of fractional charging can be circumvented. At this point, we would like to emphasise that the DFT-PC-FF method will make it possible to compute transition and reorganisation energies in charge transfer between adsorbates and the metal surface, as well as to study the problem of excited, charge state dynamics of adsorbates. In addition, since the electrons from the metal substrate do not appear explicitly in the calculation, we obtain a large decrease in computational effort, which opens up the possibility to treat large and complex systems.

As a specific system used to test the DFT-PC-FF method, we have considered the case of a gold atom on a sodium chloride bilayer supported by a copper surface. The force

field was determined from DFT calculations of a bare sodium chloride film adsorbed on the copper surface and an external uniformly charged layer in the calculations. The adsorption energies and the relaxed geometries of the gold atom in different charge states that were calculated in our new DFT-PC-FF method are compared with the results from DFT calculations of the full system. Finally, we would like to stress that the proposed DFT-PC-FF method is not limited to this specific system and could also straightforwardly be extended to other interesting systems, especially those where the ultrathin insulating film is weakly adsorbed on a metal substrate.

The paper is organised as follows. In Section 2, we describe the theory behind the development of the DFT-PC-FF method based on the PC model (Section 2.1) and how the PC model is augmented by a force field to incorporate the missing part of the interactions between the PC and the insulating film (Section 2.2). This development has required an extension of periodic DFT and DFT-PC to include an external, uniformly charged plane as described in Appendix B and Appendix C. The computational implementation and details are presented in Section 3. The explicit parameters for the PC model and the force field for a sodium chloride bilayer supported by a copper substrate are presented in Section 4.1. In Section 4.2, the DFT-PC-FF method is applied to gold adatoms in various charge states. In particular, we present results for the transition and reorganisation energies, which cannot be obtained from DFT calculations that explicitly include the metal substrate. Finally, we give some concluding remarks in Section 5.

## 2. Theory

We begin by introducing the perfect conductor model for charged adsorbates on insulating film supported by a metal substrate. Here we assume that the adsorbate is charged or discharged by the metal substrate. The PC model only includes the mean electrostatic part of the interaction, resulting in a net attractive interaction between the film and the substrate. Here we develop a simple force field that captures the residual repulsive interactions between the film and the substrate and is augmented to the PC model. Finally, we show how the the material specific parameters of our new scheme are obtained from DFT calculations of the film supported by the metal substrate. Here, we will make specific reference to a NaCl bilayer film on a Cu surface. Nevertheless, our methodology should also be applicable to other insulating films on various metal substrates.

### 2.1. The Perfect Conductor Model for Charged Adsorbates

As depicted schematically in Fig. 1 (Left), the type of systems we will consider are composed of an adsorbate (A) in different charge states adsorbed on an insulating film (IF) supported by a metal substrate (M). Throughout this work, the system will be represented in a supercell with a slab geometry of the metal substrate. The challenge

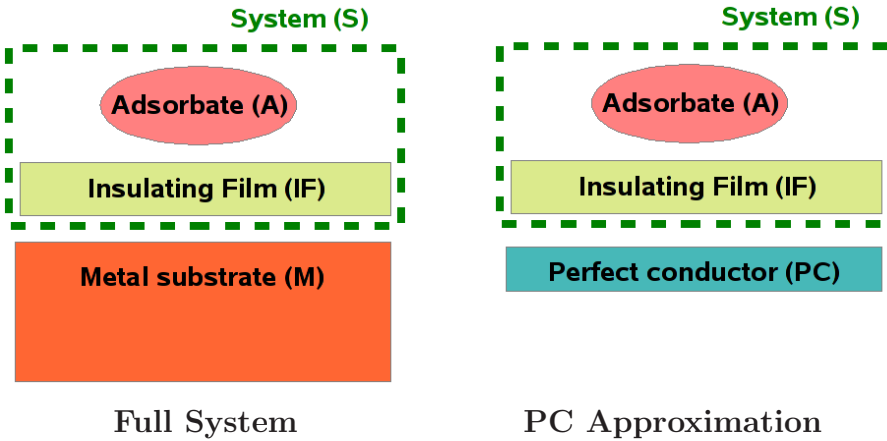


**Figure 1.** (colour online) (Left) Schematic representation of an adsorbate deposited on an insulating film supported by a metal substrate. (Right) In the perfect conductor (PC) approximation, all atoms of the metal substrate are replaced by a simple perfect conductor model. In both figures, we define the system S composed by the insulating film and the adsorbate, as indicated by the dashed line.

is to develop an approximation for the total energy  $E$  of the system M/IF/A based on the total energy  $\bar{E}$  for an external, charged and closed system (S) outside a metal surface. Here S corresponds to IF/A, as schematically shown in Fig. 1. The approximate energy functional  $\bar{E}$  was derived in our previous work [11] using the assumption that the electron densities  $n_s$  and  $n_m$  of S and M were non-overlapping, and also that non-local contributions to the exchange-correlation functional between S and M (such as van der Waals interactions between M and S) were neglected. The total energy  $\bar{E}$  is obtained by minimising the following density functional,

$$\bar{E}[n_s] = E_{m0} + E_s[n_s] + \int \rho_s(\mathbf{r})\phi_{m0}(\mathbf{r})d\mathbf{r} + \frac{1}{2} \int \rho_{ind}(\mathbf{r})\phi_s(\mathbf{r})d\mathbf{r} \quad (1)$$

with respect to  $n_s$ . Here,  $E_{m0}$  is the total energy of the isolated M,  $E_s[n_s]$  is the energy functional of the isolated S,  $\phi_{m0}(\mathbf{r})$  is the unperturbed electrostatic potential of the isolated M,  $\phi_s(\mathbf{r})$  is the electrostatic potential from the charge density of S, and  $\rho_{ind}(\mathbf{r})$  is the charge density induced by  $\phi_s(\mathbf{r})$  to linear order.  $\bar{E}[n_s]$  was derived under the assumption that S was charged from or discharged to the vacuum level but here we will now assume that the system IF/A is charged from or discharged to the Fermi level of the metal substrate M. Thus, we need to add an extra potential energy term to  $\bar{E}[n_s]$ ,

$$\tilde{E}[n_s] = \bar{E}[n_s] - Q_s \frac{\Phi}{e} \quad (2)$$

where  $Q_s$  is the charge of IF/A and  $\Phi$  is the work function of the isolated M/IF. Note that the charge  $Q_s$  is now an external parameter in Eq. (2) so that different charge states of IF/A can be treated in a controlled manner.

In the perfect conductor (PC) approximation, the explicit metal substrate is replaced by a PC model, as depicted schematically in Fig. 1 (Right). In this

approximation [11],  $\phi_{m0}(\mathbf{r})$  and  $E_{m0}$  are set to zero and the third term of Eqn.(1) vanishes. The induced charge density  $\rho_{ind}(\mathbf{r})$  in the fourth term of Eqn.(1) is localised on the PC plane and is determined by the conditions that both the electric field and the induced electrostatic potential inside the PC plane should be zero. The total induced charge at the PC plane is then equal to  $-Q_s$ , so that the total charge of the supercell is zero. Note that in applying the PC model the overlap with the electron density of IF with the PC plane cannot be avoided and it is important to use an appropriate expression for  $\rho_{ind}(\mathbf{r})$  on the PC plane that is valid for overlapping densities, as discussed in Section 2.3 of Ref. [11]. This density overlap and the neglected second term in Eqn.~(1) make it necessary to modify the work function in Eqn.~(2) so that the corresponding PC approximation of  $\tilde{E}[n_s]$  in Eq.(2) is given by,

$$\tilde{E}_{PC}[n_s] = \bar{E}_{PC}[n_s] - Q_s \frac{\Phi_{PC}}{e}, \quad (3)$$

where  $\bar{E}_{PC}[n_s]$  is the PC approximation of  $\tilde{E}[n_s]$  in Eq.(1) and  $\Phi_{PC}$  is the effective work function. The procedure to determine  $\Phi_{PC}$  is described in Section 2.3.

## 2.2. Augmentation of a Force Field to the Perfect Conductor Model

Here we develop a simple force field to approximate the energy difference,

$$\Delta E = E - \tilde{E}_{PC}, \quad (4)$$

that essentially arises from having neglected the overlapping densities and van der Waals interactions between M and S in the PC model. We will develop this force field for the IF using a the primitive surface unit cell for the M/IF system. To approximate the energy difference  $\Delta E$  in Eq. (4), we have used the following simple additive force field between the IF and the M,

$$\Delta E = \sum_{k \in NL} \phi_k(z_k) + \Delta E_0, \quad (5)$$

where the sum of the potentials  $\phi_k$  is over all atoms  $k$  of the nearest layer (NL) of the IF to the PC plane, and  $z_k$  is the perpendicular distance of atom  $k$  from this PC plane. Here,  $\Delta E_0$  is a reference energy, equal to  $\Delta E$  for M/IF in its equilibrium geometry, where  $z_k = z_{k0}$  and  $\phi_k(z_{k0}) = 0$ . Note that this equilibrium geometry is determined from the total energy  $E$ . This simple form of the force field is motivated in our case, as discussed further in Section 4, by (1) the interactions between the ions in the IF are usually much stronger than their short-ranged interactions with the M; (2) the negligible atomic relaxations of the M even in the presence of large ionic relaxations in the IF.

In the presence of an adsorbate in different charge states, we will use as a first approximation for  $\Delta E$  in Eqn. (4) the force field of Eqn. (5), but it will also be corrected by making the force field polarisable, as obtained by the introduction of a dependence of  $\phi_k$  on the system charge  $Q_s$ . This dependence arises from non-electrostatic interactions

of the IF with the screening charge in the M. The resulting approximate total energy functional  $E_{PC-FF}[n_s]$  is then given by,

$$E_{PC-FF}[n_s] = \bar{E}_{PC}[n_s] - Q_s \frac{\Phi_{PC}}{e} + \sum_{k \in NL} \phi_k(z_k, \sigma) + N_{sc} \Delta E_0(\sigma), \quad (6)$$

where  $N_{sc}$  is the number of primitive surface unit cells within the supercell and  $\sigma = -eQ_s/N_{sc}$  is the net electron excess of IF/A per primitive surface unit cell. Note that the forces on the atoms in IF/A, as obtained from the Hellman-Feynman forces generated by  $\bar{E}_{PC}[n_s]$  and by the force field are consistent with the energy functional  $E_{PC-FF}[n_s]$ .

### 2.3. Material Specific Parameters

In order to apply this approximate expression for the energy functional, we need to determine the following material specific parameters in the model: the perfect conductor plane position  $z_{PC}$ , the effective work function  $\Phi_{PC}$ , the potentials  $\phi_k(z_k, \sigma)$  in the force field and the reference energy  $\Delta E_0(\sigma)$ . Here, we use the classical image plane position  $z_{im}$  for  $z_{PC}$ . According to Lang and Kohn[17, 18, 19],  $z_{im}$  is determined by the linear density response of the conduction electrons in the bare metal surface to an external homogeneous electric field. To obtain this density response we have used a slab that represents the metal surface in a supercell, as described and calculated explicitly for the Cu(100) surface in Appendix A. Clearly, the position of the image plane will depend on the metal substrate and its orientation.

The difference between the effective PC workfunction  $\Phi_{PC}$  and the work function  $\Phi$  of the isolated M/IF is due the overlap of the electron density of IF with the PC plane, which gives rise to a potential difference between the PC plane and the vacuum level and is readily obtained from the calculated electrostatic potential.

Here, the non-electrostatic interactions of the IF with the adsorbate-induced screening charge in the M that gives rise to dependence of  $\Delta E_0(\sigma)$  and the potentials  $\phi_k(z_k, \sigma)$  on  $\sigma$  has been estimated from calculations of  $E$  and  $\tilde{E}_{PC}$  for M/IF and PC/IF, respectively, where this screening charge is approximated by the one obtained from an external, uniformly charged plane with charge  $-e\sigma$ . These calculations have required us to extend DFT and also DFT-PC to include such a charged plane in a supercell geometry. This extension with corresponding modifications of  $E$  and  $\tilde{E}_{PC}$  are described in Appendix B and Appendix C. Details of this implementation in the VASP code are presented in Appendix D. In these calculations, the reference geometries of M/IF and PC/IF are determined by the equilibrium geometry obtained from the DFT calculations for a surface primitive cell of M/IF. Similarly, the potentials  $\phi_k(z_k, \sigma)$  in Eq.(6) are obtained by calculating  $E$  and  $\tilde{E}_{PC}$  in the presence of this charged plane as a function of  $z_k$  by keeping all other atoms than atom  $k$  fixed at the reference geometry.

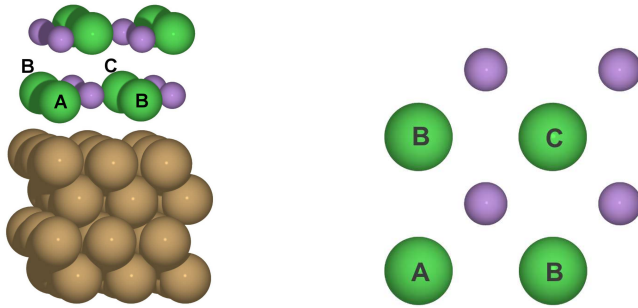


**Figure 2.** (colour online)(Left) Slab representation of a primitive surface unit cell of a NaCl bilayer supported by a Cu(100). (Right) Top view of the nearest NaCl layer to the Cu surface. Chlorine atoms (green) are labelled with letters that identify their different environments with respect to the Cu(100) substrate. In contrast, all Na atoms (violet) were found to be equivalent with respect to the substrate atom environment.

### 3. Computational implementation and details

All the DFT computations in this work including those based on the PC model have been performed using the plane wave code VASP [20]. The implementation of the PC model in VASP has been described in our previous work [11], whereas the DFT implementation of a system interacting with an external charged plane is described in Appendix D. The electron-ion interactions were handled using the projector augmented wave method (PAW) [21] and the electronic exchange and correlation effects were treated using the optB86b version [24, 25] of the van der Waals density functional. The plane wave cut-off energy was set to 400 eV.

Given the close match 2:3 of the NaCl and Cu lattice constants, the NaCl film is nearly commensurate with the Cu surface. Accordingly, the corresponding primitive surface unit cell of the NaCl bilayer supported by a Cu(100) substrate the system consists of two NaCl layers, each layer with four Na and Cl atoms, whereas the Cu(100) substrate is modelled by four layers with 9 Cu atoms in each layer, as shown in Figure 2 (Left). The interatomic distances of the Cu atoms in the two fixed bottom layers were kept at the calculated bulk distances of 2.546 Å [26].

In the calculations behind the determination of the force field, the supercell contained a single surface unit cell and the Brillouin zone was sampled by  $4 \times 4 \times 1$  k-points. For the calculations of the neutral and charged Au adatom, we have used supercells containing  $2 \times 2$  and  $3 \times 3$  surface unit cells, with Brillouin zone sampling of  $2 \times 2 \times 1$  and  $1 \times 1 \times 1$  k-points, respectively. All ionic relaxations were carried out until the magnitude of the forces were smaller than 0.02 eV/Å. In the calculations using an external, uniformly charge plane, the position of this plane was set at an average distance of 2.8 Å with respect to the top NaCl layer.

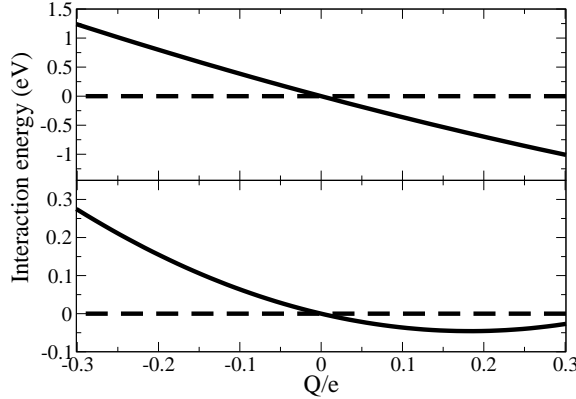


**Figure 3.** Quadratic fits to calculated interaction energies  $E^{int}[Q] = E[Q] - E[Q = 0]$  (Upper panel) for a single surface unit cell of NaCl(2ML)/Cu(100) and  $\bar{E}_{PC}^{int}[Q] = \bar{E}_{PC}[Q] - \bar{E}_{PC}[Q = 0]$  (Lower panel) for a single surface unit cell of NaCl(2ML)/PC both interacting with an external, uniformly charged plane as a function of its charge  $Q$ .

## 4. Results

We start by determining the material specific parameters and the force field in the DFT-PC-FF method based on DFT calculations of a bare NaCl bilayer on a Cu(100) surface. The derived force field is then used with the DFT-PC-FF method to compute the total energy and geometric structure of neutral and negatively charged states of a Au adatom. In particular, we are now able to calculate transition and reorganization energies.

### 4.1. NaCl bilayer supported by a Cu(100) surface: force field

The equilibrium geometry for the primitive surface unit cell of the NaCl bilayer on the Cu(100) surfaces (Fig 2 (Left)) is determined from DFT calculations including the metal substrate. From the relaxed ionic positions of the nearest NaCl layer to the Cu(100) substrate, we find that the four sites for the Na cations are equivalent with respect to the substrate atom environment. In contrast, only two sites of the four Cl anions are equivalent and are differentiated by assigning different labels to each inequivalent Cl anion, as shown in Fig. 2. Furthermore, we find that the geometrical relaxations of the Cu substrate atoms are small compared to the bare surface. In fact, the standard deviation of the  $z$  coordinates for the displacements of the Cu atoms of the outer metal layer is about 0.04 Å. Thus, we can assume that all Cu atoms of the outer layer are located in the same plane, and use the image plane position  $z_{im}$  of the bare substrate to approximate the electrostatic response of metal substrate. The details of the calculations of  $z_{im}$  for the bare Cu(100) surface using a slab representation of the surface is described in Appendix A. We find that  $z_{im}$  is converged when increasing the number of Cu layers to 13 and  $z_{im} = 1.48$  Å with respect to the plane of the outermost Cu layer ( $z=0$ ).

The next step is to determine the effective work function  $\Phi_{PC}$  in the PC model and

the reference energy  $\Delta E_0(\sigma)$ . To this end, we will use the reference geometry for the IF/M to be the equilibrium geometry above for the primitive surface unit cell. For this reference geometry, we will compute the interaction energy  $E^{\text{int}}[Q] = E[Q] - E[Q = 0]$  of the NaCl bilayer on the Cu(100) slab with an external, uniformly charged plane with charge  $Q = -e\sigma$ , and the corresponding interaction energy  $\bar{E}_{\text{PC}}^{\text{int}}[Q] = \bar{E}_{\text{PC}}[Q] - \bar{E}_{\text{PC}}[Q = 0]$  in the PC model of the Cu(100) slab. As shown in Fig. 3, the computed interaction energies as a function of  $Q$  are very well approximated by a quadratic function,

$$F[Q] = -W \frac{Q}{e} + \frac{Q^2}{2C}. \quad (7)$$

Here the linear term  $W\delta Q/e$  corresponds to the energy required to transfer an infinitesimal charge  $\delta Q$  from the system to the vacuum region and  $C$  is the capacitance. In the full DFT calculation,  $W_F$  is simply to equal to the work function  $\Phi$ , since the external plane is charged from the Fermi level of the metal substrate. From the quadratic fit to the computed  $E^{\text{int}}[Q]$  we obtain  $W_F = 3.74$  eV. This value is indeed very close to the calculated value for  $\Phi = 3.73$  eV obtained from the computed Fermi energy with respect to the vacuum level.

In contrast,  $W_{\text{PC}}$  differs from  $\Phi$  in the PC approximation, since the derivation of this approximation is based on charging from the vacuum level. In this latter case, as shown in Appendix E,  $W_{\text{PC}}$  is given by the electrostatic potential energy difference  $e\Delta\phi$  between the vacuum level and the PC plane. Here, the extracted value for  $W_{\text{PC}} = 0.501$  eV from the corresponding fit to  $\bar{E}_{\text{PC}}^{\text{int}}[Q]$  is close to the calculated value  $e\Delta\phi = 0.526$  eV. The effective work function in the PC model is then given by  $\Phi_{\text{PC}} = W_F - W_{\text{PC}} = 3.74 - 0.50 = 3.24$  eV.

The calculated capacitance  $C_{\text{PC}} = 0.365$  e/V in the PC model is about 8% smaller than the capacitance  $C_F = 0.395$  e/V in the full DFT calculation and could be corrected by adjusting the position of the perfect conductor plane but that has not been attempted here. Now, using Eq. (4) and the quadratic form for the interaction energies in Eq. (7), the reference energy per primitive surface unit cell  $\Delta E_0(\sigma)$  is given by,

$$\Delta E_0(\sigma) = \Delta E_0 + \left[ \frac{1}{C_F} - \frac{1}{C_{\text{PC}}} \right] \frac{(e\sigma)^2}{2}. \quad (8)$$

The linear term in  $\sigma$  vanishes since  $\Phi_{\text{PC}} = W_F - W_{\text{PC}}$ .

The final step is to determine the potentials  $\phi_k(z_k, \sigma)$  in the force field in Eqn.(6) from how the energy  $\Delta E(\sigma)$  in Eqn.(4) changes for the atoms of the NaCl bilayer with respect to the their distances to the PC plane and  $\sigma$ . Here, we have assumed that these potentials only affects the atoms of the nearest layer to the metal surface, and has a dependence on the atom kind and its atomic site. The inequivalent sites of the Cl anions and Na cations with respect to substrate atoms, were identified according to the labelling of Fig. 2. The calculation of  $\Delta E(\sigma) - \Delta E_0(\sigma)$ , for different values of  $z_k$  and  $\sigma$  leads to various energy profiles that decay rapidly with the distance to the PC plane. To fit the computed set of data, we have used Morse functions

$$\phi_k(z_k, \sigma) = A_{k0} [1 - e^{-A_{k1}(z_k - A_{k2})}]^2 + A_{k3} \quad (9)$$

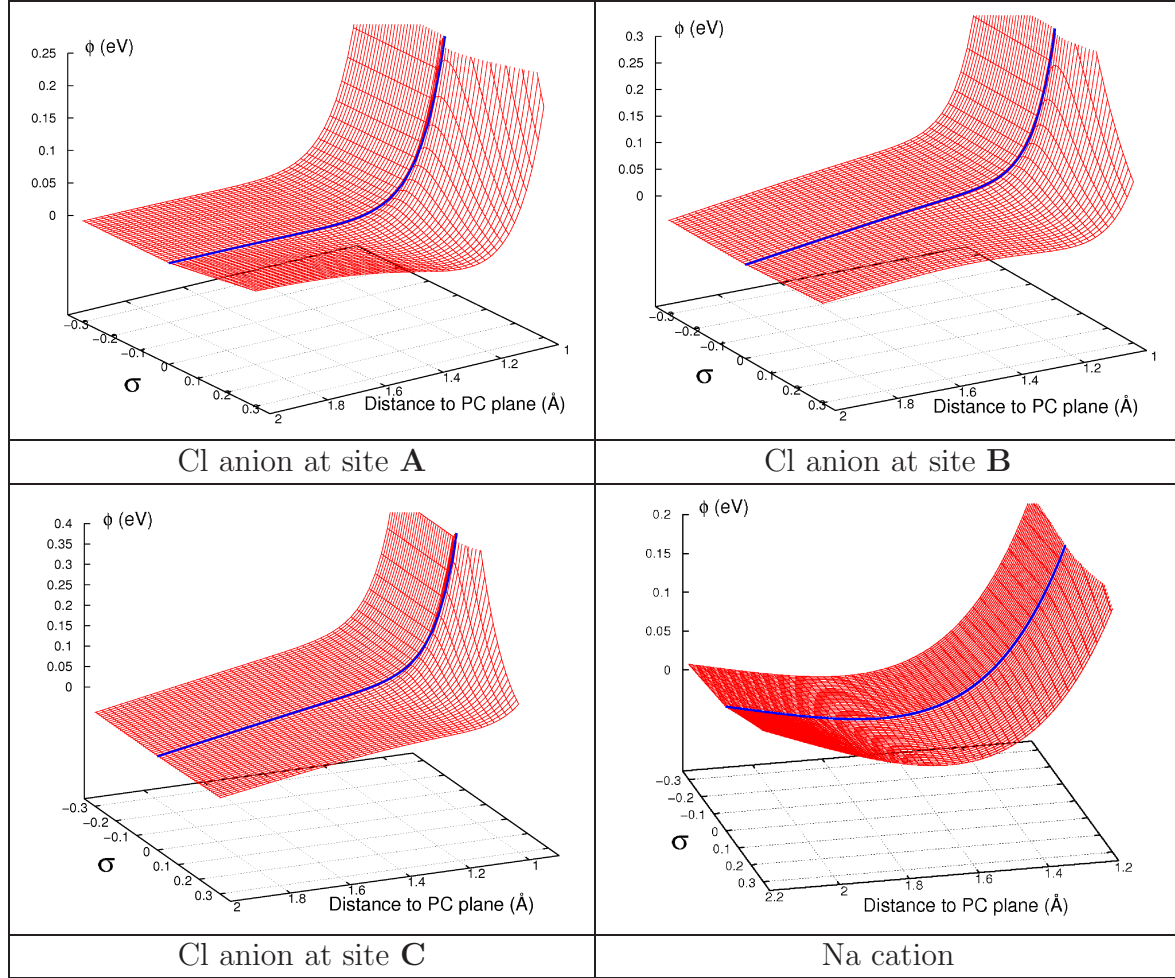


**Figure 4.** (colour online) Calculated potentials  $\phi$  as a function of the atom distance  $z$  to the PC plane and the charge  $e\sigma$  per surface unit cell, for each atom of the NaCl layer as labelled in Fig. 2 (Right). The solid lines are the results for  $\sigma = 0$ .

where each coefficient  $A_{k,i}$  is at most a quadratic function of  $\sigma$ . Figure 4 shows the results of the fitting of  $\phi$  for each atom, as a function of  $\sigma$  and the distance  $z_k$  to the PC plane inside the surface unit cell. In addition, we show by the solid line the potential  $\phi$  for  $\sigma=0$ . As expected, we find that the potential increases when either the Na or Cl atom approaches to the image plane, and has a weak dependence on the charge  $e\sigma$  induced at the PC. In fact, the presence of this charge will polarise the NaCl bilayer, such that the ions will relax to a slightly different configuration. The use of Morse-like functions to fit the data indicates that the potentials are not purely repulsive, but they also exhibit small attractive contributions, mainly for  $z_k$  close to their equilibrium values. In the following, we will refer to  $\phi_k(z_k, \sigma)$  and  $\phi_k(z_k, \sigma = 0)$  as polarised and non-polarised potentials, respectively.

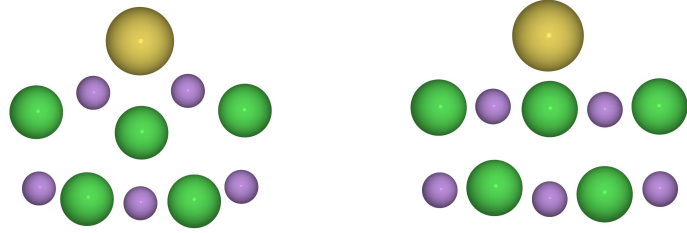


**Figure 5.** (colour online) Side view of the computed geometries for the negative (Left) and the neutral (Right) Au atom (yellow) and Cl (green) and Na (violet) ions. For both charge states, the Au adatom is situated in top of a Cl anion. Whereas the negative Au ( $\text{Au}^-$ ) adatom results in large relaxations of the NaCl bilayer, the neutral charge state ( $\text{Au}^0$ ) of the Au adatom leaves the bilayer almost unaffected.

#### 4.2. Charge states of an Au adatom on a NaCl bilayer supported by a Cu(100) surface

Our proposed approximate DFT-PC-FF method will now be illustrated and tested by presenting results for the neutral and negatively charged Au adatom on a NaCl bilayer supported by a Cu(100) substrate. The quality of this method is judged by comparing calculated values of adsorption energies and relaxed structures with available results from DFT calculations that include the explicit Cu(100) substrate, from now on referred to as DFT-FULL. Furthermore, we present results for the vertical transition energy for charging the Au adatom and the associated reorganisation energy, which cannot be obtained from DFT-FULL calculations. For the DFT-PC-FF simulations, we have considered supercells composed of  $2 \times 2$  and  $3 \times 3$  primitive surface units cells, being this surface unit cell as previously defined in Fig. 2. For the DFT-FULL computations we have only considered supercell with the  $2 \times 2$  primitive surface unit cells.

Previous STM experiments combined with DFT calculations showed that the Au adatom has two possible charge states, either being negatively charged or neutral, and each charge state result in a very different ionic relaxations of the NaCl film [3]. The ionic relaxation in the DFT-FULL calculation, where only the two bottom Cu layers are fixed, results in a negatively charged Au adatom situated on top of a Cl anion and a large ionic relaxations of the NaCl layer, as schematically shown in Fig. 5 (Left). Due to the electrostatic interactions, the Cl anion coordinated to the Au anion is pushed towards the bottom NaCl layer, while the four surrounding Na cations ions are pulled outwards, in agreement with the results in Ref. [3]. In contrast to the large ionic relaxations of the NaCl bilayer, we find that the relaxations of the Cu substrate atoms are small and negligible. In fact, when keeping the Cu substrate atoms at their positions in the absence of an adsorbate, we find that the resulting total energy is only 0.03 eV larger than the total energy when the two outer most Cu(100) layers are allowed to relax. The negligible role of the small substrate relaxations justifies our simple force field model with potentials that only depend on the distance from the image plane position. Henceforth, all the DFT-FULL calculations have been carried out by fixing the Cu(100) layers to their equilibrium positions of the bare NaCl bilayer.

	DFT-FULL	DFT[3]	DFT-PC-FF	
supercell size	$2 \times 2$	$2 \times 2$	$2 \times 2$	$3 \times 3$
<b>Au<sup>-</sup></b>				
$d_{\text{Au}-\text{Cl}}(\text{\AA})$	3.34	3.4	3.32 (3.35)	3.31 (3.32)
$E_{\text{ads}}(\text{eV})$	1.37	1.1	1.20 (1.27)	1.21 (1.28)
<b>Au<sup>0</sup></b>				
$d_{\text{Au}-\text{Cl}}(\text{\AA})$	–	3.2	2.53	2.53
$E_{\text{ads}}(\text{eV})$	–	0.4	0.64	0.68

**Table 1.** Calculated adsorption energies  $E_{\text{ads}}$  and the distance  $d_{\text{Au}-\text{Cl}}$  from the Au atom to the Cl anion for each charge state of the Au adatom, when including the explicit Cu(100) substrate in the DFT calculations (DFT-FULL), previous DFT results [3] and when using the new DFT-PC-FF method. Values in parenthesis show the resulting values when using the polarisable potentials  $\phi_{\mathbf{k}}(z_{\mathbf{k}}, \sigma_s)$  in the force field.

We now turn to the computation of the negatively charged Au adatom using the DFT-PC-FF method. This state is now simply obtained by adding one electron to the NaCl bilayer and the Au adatom. The added electron will induce an equal but opposite charge at the PC plane, which ensures the neutrality of the supercell. The resulting values for the adsorption energy and the distance between the Au atom and the Cl atom underneath are shown in Table 1. Results for DFT-PC-FF with the polarisable force field are shown in parenthesis. In agreement with the DFT-FULL calculations, we obtain a very similar relaxed geometric structure. In fact, for the  $2 \times 2$  supercell a DFT-FULL calculation using the relaxed geometrical structure from the DFT-PC-FF calculation with the non-polarisable force field gives an adsorption energy of 1.26 eV, which differ only by 0.11 eV from the adsorption energy 1.37 eV for the fully relaxed geometrical structure in the DFT-FULL calculation. Instead, if we use the relaxed structure obtained with the polarisable force field then the difference in the adsorption energy reduces from 0.11 eV to 0.04 eV. Furthermore, a comparison with the results from the DFT-FULL calculations shows that DFT-PC-FF gives a minor difference in the Au-Cl interatomic distance, always smaller than 0.02 Å, independently if the force field is polarisable or not. Finally, the adsorption energy is underestimated by about 0.17 eV (14%) compared to DFT-FULL when using the non-polarisable potentials  $\phi_{\mathbf{k}}(z_{\mathbf{k}})$ , but is underestimated by only 0.10 eV (8%) when using the polarisable potentials  $\phi_{\mathbf{k}}(z_{\mathbf{k}}, \sigma)$ . Note that there is a huge reduction in the computational time with about two orders of magnitude in the DFT-PC-FF calculations compared to the DFT-FULL calculations.

The negatively charge state for the Au adatom is readily obtained in our DFT-FULL calculations, whereas we have not been able to identify a neutral state. In the DFT calculations reported in [3], they were able to identify a neutral-like state that had a small fractional charge. In contrast, the DFT-PC-FF method provides a simplified and efficient way to compute all those charge states that standard DFT has a hard time or fails to predict. To obtain the neutral charge state of the Au adatom in the

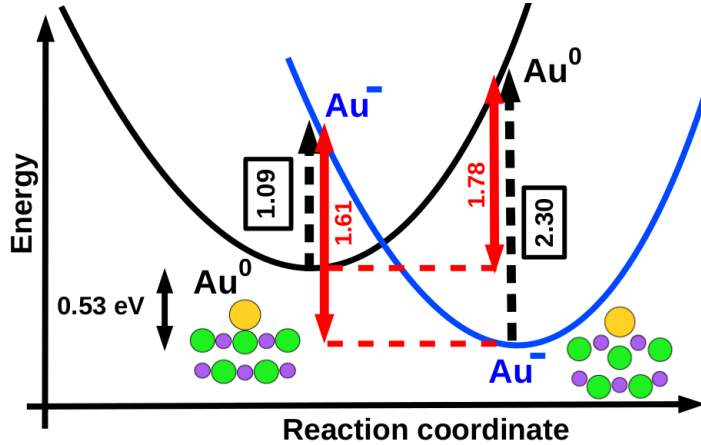


**Figure 6.** (colour online) Simple Marcus picture of charging and discharging of the Au adatom on the NaCl bilayer supported by a Cu(100) surface. The parabola indicate schematically the diabatic potential energy curves as a function of the reaction coordinate. The vertical transition energies (dashed lines) and reorganisation energies (solid lines) are also indicated as calculated using the DFT-PC-FF method. The results were obtained for a  $3 \times 3$  supercell and a non-polarisable potential.

DFT-PC-FF method, we simply set the charge of the NaCl bilayer and the Au adatom to zero. In contrast to the negative Au atom, we find that the NaCl bilayer is almost unaffected by the presence of the neutral Au adatom, as schematically shown in Fig. 5 (Right), in agreement with the earlier calculations in Ref. [3]. In comparison with the negative charge state of the Au adatom, the neutral Au adatom is 0.8 Å closer to the Cl anion and has a smaller adsorption energy. Although, the presented results are in agreement with those published in Ref. [3], we obtain some differences in the calculated values, because van der Waals interactions were included in our calculations. Finally, note that the results in DFT-PC-FF are essentially converged for the  $2 \times 2$  supercell since they are very close to the results for the  $3 \times 3$  supercell.

In the STM experiments for the charging of an Au adatom on a NaCl bilayer supported by a Cu(111) surface, an analysis of the observed switching rate with bias suggested that the charging occurred by tunnelling electron attachment to a  $\text{Au}^-$  adatom state at about 1.4 eV. This vertical transition energy is given by the energy to charge the Au adatom in the equilibrium structure of the NaCl bilayer with the neutral Au adatom. This anionic state cannot be realised in the DFT-FULL calculations since it is an electronically excited state for this structure. However, this anionic state is an electronic ground state in the DFT-PC-FF scheme in the presence of an extra electron. Furthermore, with DFT-PC-FF we can also calculate the vertical transition energy for neutralising the  $\text{Au}^-$  adatom given by the energy difference between the neutral Au adatom and the  $\text{Au}^-$  adatom in the equilibrium structure of the NaCl bilayer and the Au adatom. In Fig. 6, we show the calculated values for these two transition energies in a diagram that also shows the similarities of this charging and discharging mechanisms to the classical Marcus picture for electron transfer with schematic diabatic potential

energy curves. From the calculated transition and the adsorption energies of the neutral and charged adatom in Table 1, we also obtain directly the reorganisation energies in this picture associated with the geometrical relaxations of NaCl bilayer for charging and discharging. The calculated values of these energies are also shown in Fig. 6 and are rather close to each other. In fact, these energies should be equal in a simple linear ionic and electron response model for the NaCl bilayer on the Cu substrate to the adatom charge.

In order to compare the calculated transition energy for charging of the Au adatom with the experimental value, we need to correct for the workfunction difference for the supported NaCl bilayer when changing the substrate from Cu(100) to Cu(111). This workfunction difference is about 0.35 eV larger than when using the Cu(111) substrate [27], so according to Eq.(6), we have to shift the energies of the  $\text{Au}^-$  adatom in Fig. upwards with about 0.35 eV. This changes the transition energy for charging of the Au adatom from 1.09 eV to 1.44 eV in close agreement with the value of 1.4 eV suggested by experiments.

## 5. Concluding remarks

The applicability of periodic density functional theory (DFT) methods to calculate the total energy and forces of charged adsorbates on ultra-thin insulating films, supported by a metal substrate, are severely limited by the inherent delocalisation error of current exchange-correlation functionals. Here, we have developed and presented a simplified and efficient DFT method that surmounts this limitation. This new DFT-PC-FF method is based on the perfect conductor (PC) model to approximate the electrostatic response of the metal substrate, while the film and the adsorbate are both treated fully within DFT. The missing interactions between the metal substrate and the insulating film in the PC model are modelled by a simple force field (FF). The parameters of the PC model and the force field are obtained from DFT calculations of the film and the substrate. In order to obtain some of these parameters and the polarisability of the force field, we have to include an external, uniformly charged plane in the DFT calculations, which has required the development of an extension of periodic DFT to include such a charged plane within a supercell. An extension that should be of more general interest and applicable to other challenging problems, for instance, in electrochemistry. The developed DFT-PC-FF method allows us to handle the different charge states of adsorbates in a controlled manner. Another most important advantage of this new scheme is the large reduction in computer time and memory, since the metal electrons are not explicitly included in the calculation.

The proposed DFT-PC-FF method is illustrated and tested by considering the specific case of a NaCl bilayer, which is supported by a Cu(100) substrate. We have carried out calculations for neutral and charged Au adatoms on this film and compared the results with results from DFT calculations that explicitly include the Cu(100) substrate, although such a comparison was not possible for every charge state. In

addition, we have calculated the vertical transition energy for charging the Au adatom and obtain a close agreement with the value suggested by experiments. These energies cannot be obtained from DFT calculations that include the full metal substrate.

Our results show that the DFT-PC-FF method not only predicts encouraging results for adsorption and transition energies and relaxed structures of charged adsorbates, but also reduces considerably the computational time by a factor of almost two orders of magnitude. In fact, the possibility to perform efficient DFT simulations by controlling the charge state of adsorbates will allow to study various physical processes and properties, which are currently either extremely challenging or not possible due to the charge delocalisation error. In this respect, some interesting problems involving insulating polar films we plan to address in the near future are the following: (1) calculation of diffusion barriers for adsorbates in various charge states; (2) HOMO-LUMO gaps of molecular complexes; (3) molecular dynamics simulations of bond formation and breaking upon charging and discharging.

## Acknowledgments

The authors acknowledge Leverhulme Trust for funding this project through the grant (F/00 025/AQ) and allocation of computer resources at HECToR through the membership in the materials chemistry consortium funded by EPSRC (EP/F067496) and at Lindgren, PDC through SNIC. Mats Persson is grateful for the support from the EU project ARTIST.

## Appendix A. Calculation of the image plane for Cu(100)

The calculations of the position  $z_{im}$  of the image plane follows the classical work by Lang and Kohn [19], where this position with respect to outer most surfaces layer is given by the centroid of the induced charged density  $\rho_{ind}(\mathbf{r})$  by an external homogeneous electric field as,

$$z_{im} = \frac{\int z \rho_{ind}(\mathbf{r}) d\mathbf{r}}{\int \rho_{ind}(\mathbf{r}) d\mathbf{r}} + \frac{D}{2}, \quad (A.1)$$

where  $D$  is the interlayer separation. In this work,  $\rho_{ind}(\mathbf{r})$  has been calculated using VASP using the standard implementation of an external, homogeneous field by an external surface dipole layer. To model the Cu surface, we have used a slab geometry and gone up to 15 Cu layers with a vacuum region of 20 Å. Each layer contains a single Cu atom and the interatomic distance was set to the calculated bulk value of 2.546 Å. The exchange-correlation effects were described by the PBE functional and the ion-core interactions using the PAW. The Brillouin zone was sampled by  $11 \times 11 \times 1$   $k$  point grid. Since the external electric field is applied on both sides of the slab,  $\rho_{ind}(\mathbf{r})$  becomes anti-symmetric, as shown in Fig. A1, and the net induced charge is zero. In order to approximate a semi-infinite surface, the centroid of  $\rho_{ind}(\mathbf{r})$  in Eq.(A.1) was evaluated by integrating  $\rho_{ind}(\mathbf{r})$  to the centre of the slab. As also shown in Fig. A1, the induced

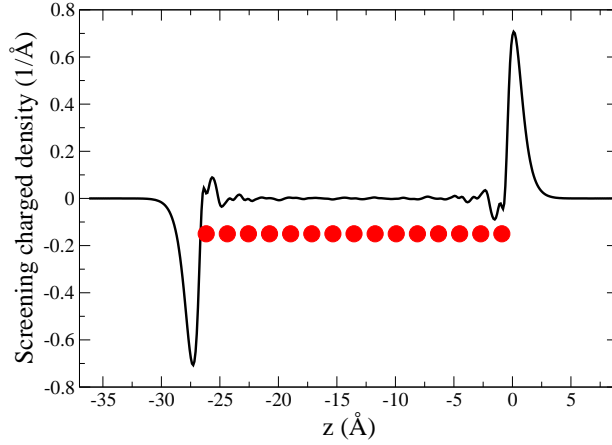


**Figure A1.** (colour online) Laterally average of induced charge density  $\rho_{\text{ind}}(\mathbf{r})$  along the  $z$  d

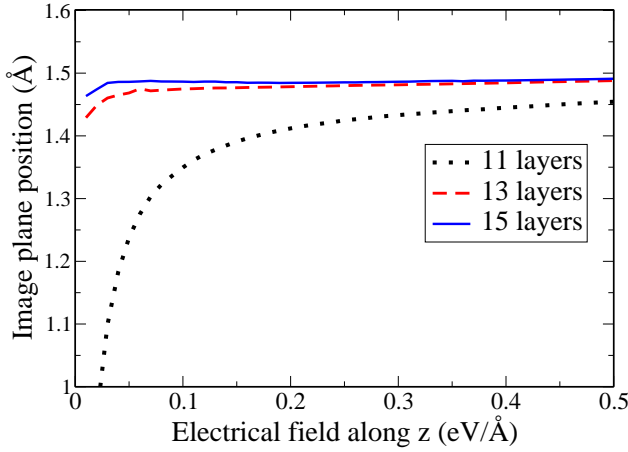


**Figure A2.** (colour online) Position of the image plane as a function of the applied electrical field and for slabs with different number of Cu layers.

charge density has weak, long-range Friedel oscillations into the bulk, so it is necessary to increase the number of Cu layers to at least 13 to get a converged result for different strengths of the external electric field (Fig. A2). Note that the small deviations in the region of small electrical fields for the slabs composed of 13 and 15 layers is expected and caused by numerical cancellation errors in determining  $\rho_{\text{ind}}(\mathbf{r})$ .

## Appendix B. Modification of the energy functional in the presence of an external, uniformly charged plane

In this section, we derive how the total energy functional in density functional theory is modified for a system  $S$  in the presence of an external, uniformly charged plane (UCP) with a total charge  $Q_{\text{ext}}$  located at a position  $z = z_{\text{ext}}$ . The system  $S$  and the UCP is represented in a supercell and  $S$  is assumed to include a metal substrate so that the total induced charge in  $S$  is  $Q_s = -Q_{\text{ext}}$  and the super cell is neutral. Here,

$L_z$  is the length of the supercell along the perpendicular ( $z$ ) direction to the metal substrate and  $A$  is its cross sectional area. The electrostatic potentials of the charge density  $\rho_{\text{ext}}(\mathbf{r}) = \frac{Q_{\text{ext}}}{A}\delta(z - z_{\text{ext}})$  of UCP and the charge density  $\rho_s(\mathbf{r})$  of the system S in the supercell are denoted by  $\phi_{\text{ext}}(\mathbf{r})$  and  $\phi_s(\mathbf{r})$ , respectively. The UCP will only affect directly the electrostatic part  $E_{\text{el,UCP}}[n_s]$  of the total energy functional, whereas the kinetic energy and the exchange correlation functionals remain unaffected. With this,  $E_{\text{el,UCP}}[n_s]$  is given by

$$E_{\text{el,UCP}}[n_s] = \frac{1}{2} \int_V \rho_s(\mathbf{r}) \phi_s(\mathbf{r}) d\mathbf{r} + \int_V \rho_s(\mathbf{r}) \phi_{\text{ext}}(\mathbf{r}) d\mathbf{r} + \frac{1}{2} \int_V [\rho_s + \rho_{\text{ext}}](\mathbf{r}) \phi_{\text{dip}}(z) d\mathbf{r}. \quad (\text{B.1})$$

where the dependence on  $Q_{\text{ext}}$  has been indicated. Here the first term on the RHS is the electrostatic self-interaction energy of the charge density  $\rho_s(\mathbf{r})$ , the second term is the electrostatic interaction energy between  $\rho_s(\mathbf{r})$  and  $\rho_{\text{ext}}(\mathbf{r})$ , and the last term is the dipole energy correction. The latter dipole term corrects for the effects on the electrostatic potential from the periodic boundary conditions in the  $z$  direction, as discussed by Neugebauer and Scheffler [29] and later corrected by Bengtsson [30]. The dipole potential  $\phi_{\text{dip}}(z)$  is generated by a uniform surface dipole layer with a surface dipole  $-m$  determined by the total perpendicular dipole moment of total charge distribution:

$$m = \frac{1}{A} \int_V \rho_s(\mathbf{r}) z d\mathbf{r} + \frac{z_{\text{ext}} Q_{\text{ext}}}{A}. \quad (\text{B.2})$$

In the case when the dipole layer is located at  $z = L_z$ , the dipole potential is given by,

$$\phi_{\text{dip}}(z) = 4\pi m \left[ \frac{z}{L_z} - \frac{1}{2} \right], \quad 0 < z < L_z. \quad (\text{B.3})$$

The functional derivative of Eq. (B.1) with respect to the electronic density  $n_s(\mathbf{r})$  gives the dipole-corrected electrostatic part  $\phi_{\text{UCP}}(\mathbf{r})$  of the K-S potential

$$\phi_{\text{UCP}}(\mathbf{r}) = \phi_s(\mathbf{r}) + \phi_{\text{ext}}(\mathbf{r}) + \phi_{\text{dip}}(z). \quad (\text{B.4})$$

Thus, the only modification of the K-S potential is that its electrostatic part is replaced by  $\phi_{\text{UCP}}(\mathbf{r})$  given in Eq.(B.4). Furthermore, the same replacement needs to be done in the calculation of the Hellman-Feynman forces. Usually, the kinetic energy is calculated from the one-electron sum, which generates double counting terms. In this case only the double counting term  $E_{\text{el,UCP}}^{\text{DC}}$  from the electrostatic energy is modified and is given by,

$$E_{\text{el,UCP}}^{\text{DC}}(Q_{\text{ext}}) = - \int_V \rho_e(\mathbf{r}) [\phi_s(\mathbf{r}) + \phi_{\text{ext}}(\mathbf{r}) + \phi_{\text{dip}}(z)] \quad (\text{B.5})$$

where  $\rho_e(\mathbf{r}) = -en_s(\mathbf{r})$ . Adding this term to the dipole-corrected electrostatic energy of Eqn. (B.1), one obtains,

$$\begin{aligned}
[E_{el,UCP} + E_{el,UCP}^{DC}](Q_{ext}) = & -\frac{1}{2} \int_{\mathcal{V}} \rho_e(\mathbf{r}) \phi_e(\mathbf{r}) d\mathbf{r} + \\
& \frac{1}{2} \int_{\mathcal{V}} \rho_i(\mathbf{r}) \phi_i(\mathbf{r}) d\mathbf{r} + \\
& \frac{1}{2} \int_{\mathcal{V}} [\rho_i - \rho_e - \rho_{ext}](\mathbf{r}) \phi_{dip}(z) d\mathbf{r} + \\
& \int_{\mathcal{V}} \rho_{ext}(\mathbf{r}) [\phi_i(\mathbf{r}) + \phi_{dip}(z)] d\mathbf{r}
\end{aligned} \tag{B.6}$$

where  $\phi_i$  is the electrostatic potential from the ionic charge charge density  $\rho_i(\mathbf{r})$  in the supercell. Note that the integrals over the supercell are carried out in reciprocal space by excluding the  $\mathbf{g} = 0$  component.

### Appendix C. Modification of the PC energy functional in the presence of an external, uniformly charged plane

In this Section, we derive how the total energy functional is modified in the case of perfect conductor (PC) model of the metal substrate and an external closed system  $S$  in the presence of an external, uniformly charged plane (UCP) with a total charge  $Q_{ext}$  located at a position  $z = z_{ext}$ . In this case, the system  $S$  can have a net charge  $Q_s$ . For further details of the formalism behind the PC model, we refer the reader to Ref. [11]. As in the previous case only the electrostatic contribution to the total energy functional and consequently the K-S potential will be modified by the UCP. The presence of the UCP and  $S$  will induce a charge density at the perfect conductor plane located at  $z = z_{PC}$  and is defined as,

$$\rho_{ind}(\mathbf{r}) = \sigma_{ind}(\mathbf{R}) \delta(z - z_{PC}). \tag{C.1}$$

The laterally-averaged, induced surface charge density  $\bar{\sigma}_{ind}$  screens completely the total charge of UCP and  $S$ , and is given by,

$$\bar{\sigma}_{ind} = -\frac{(Q_s + Q_{ext})}{A}, \tag{C.2}$$

and the laterally varying part of the surface charge density  $\sigma'_{ind}(\mathbf{r})$  is determined by the electrostatic potential  $\phi_s(\mathbf{r}) + \phi_{ext}(\mathbf{r})$  from  $\rho_s(\mathbf{r}) + \rho_{ext}(\mathbf{r})$  and in reciprocal space it is given by,

$$\sigma_{ind}(\mathbf{G}) = -\frac{G}{2\pi} [\phi_s + \phi_{ext}](z_{PC}, \mathbf{G}), \tag{C.3}$$

for non-zero reciprocal lattice vectors ( $\mathbf{G} \neq 0$ ) of the supercell, following the notation of Ref. [11]. Note that the  $\mathbf{G} = 0$  component of  $\sigma_{ind}$  is equal to  $\bar{\sigma}_{ind}$ . The electrostatic energy,  $E_{el,UCP}^{PC}$ , of the system  $S$  interacting with the PC and the external charge plane UCP is then given by,

$$E_{el,UCP}^{PC}(Q_{ext}) = \frac{1}{2} \int_{\mathcal{V}} \rho_s(\mathbf{r}) \phi_s(\mathbf{r}) d\mathbf{r} +$$

$$\begin{aligned} & \int_{\mathcal{V}} \rho_s(\mathbf{r}) \phi_u(\mathbf{r}) d\mathbf{r} + \frac{1}{2} \int_{\mathcal{V}} [\rho_s + \rho_{\text{ext}}](\mathbf{r}) \phi_{\text{dip}}(z) d\mathbf{r} + \\ & \frac{1}{2} \int_{\mathcal{V}} \rho_{\text{ind}}(\mathbf{r}) [\phi_s + \phi_{\text{ext}}](\mathbf{r}) d\mathbf{r} \end{aligned} \quad (\text{C.4})$$

whose form differs from Eqn. (B.1) by the electrostatic interaction of  $\rho_{\text{ind}}(\mathbf{r})$ , with the charge of  $S$  and UCP. The dipole potential  $\phi_{\text{dip}}(z)$  has been previously defined in Eqn. (B.3) but the surface dipole moment  $m$  in Eq. B.2 now contains also a contribution from  $\rho_{\text{ind}}(\mathbf{r})$ ,

$$m = \frac{1}{A} \int_{\mathcal{V}} [\rho_s + \rho_{\text{ind}}](\mathbf{r}) z d\mathbf{r} + \frac{z_{\text{ext}} Q_{\text{ext}}}{A}. \quad (\text{C.5})$$

Rearranging terms in Eqn. (C.4), we obtain

$$\begin{aligned} E_{\text{el,UCP}}^{\text{PC}}(Q_{\text{ext}}) = & \frac{1}{2} \int_{\mathcal{V}} \rho_s(\mathbf{r}) [\phi_s + \phi_{\text{ind}} + \phi_{\text{ext}} + \phi_{\text{dip}}](\mathbf{r}) d\mathbf{r} + \\ & \frac{1}{2} \int_{\mathcal{V}} \rho_u(\mathbf{r}) [\phi_s + \phi_{\text{ind}} + \phi_{\text{ext}} + \phi_{\text{dip}}](\mathbf{r}) d\mathbf{r} \\ & - \frac{1}{2} \int_{\mathcal{V}} \rho_{\text{ext}}(\mathbf{r}) \phi_{\text{ext}}(\mathbf{r}) d\mathbf{r} \end{aligned} \quad (\text{C.6})$$

where  $\phi_{\text{ind}}$  is the electrostatic potential from  $\rho_{\text{ind}}(\mathbf{r})$  in the supercell. Following the derivation in Ref. [11], the dipole-corrected electrostatic potential  $\phi_{\text{dip-corr}}(\mathbf{r}) = [\phi_s + \phi_{\text{ind}} + \phi_u + \phi_{\text{dip}}](\mathbf{r})$  within the supercell is equal, up to a constant, to the electrostatic potential from  $\rho_s(\mathbf{r})$ ,  $\rho_{\text{ind}}(\mathbf{r})$  and  $\rho_u(\mathbf{r})$  in the absence of the periodic boundary conditions in the direction perpendicular to the PC plane. Therefore, the electrostatic potential for the system  $S$ ,  $\phi_{\text{el,UCP}}^{\text{PC}}(\mathbf{r})$ , is simply obtained by adding a constant  $\phi_1$  to the dipole corrected potential,

$$\phi_{\text{el,UCP}}^{\text{PC}}(\mathbf{r}) = \phi_{\text{dip-corr}}(\mathbf{r}) + \phi_1 \quad (\text{C.7})$$

and since the lateral average  $\bar{\phi}_{\text{el,UCP}}^{\text{PC}}(\mathbf{r}z)$  of  $\phi_{\text{el,UCP}}^{\text{PC}}(\mathbf{r})$  has to be zero inside the PC,  $\phi_1$  is determined by the following condition at the PC plane

$$\phi_1 = -[\bar{\phi}_s + \bar{\phi}_{\text{ind}} + \bar{\phi}_{\text{ext}} + \bar{\phi}_{\text{dip}}](z_{\text{PC}}) \quad (\text{C.8})$$

Finally, replacing  $\phi_{\text{dip-corr}}(\mathbf{r})$  by  $\phi_{\text{el,UCP}}^{\text{PC}}(\mathbf{r})$  in Eqn. C.6, one gets the corrected expression for the electrostatic energy,

$$\begin{aligned} E_{\text{el,UCP}}^{\text{PC}}(Q_{\text{ext}}) = & \frac{1}{2} \int_{\mathcal{V}} \rho_s(\mathbf{r}) \phi_s(\mathbf{r}) d\mathbf{r} + \\ & \int_{\mathcal{V}} \rho_s(\mathbf{r}) \phi_{\text{ext}}(\mathbf{r}) d\mathbf{r} + \frac{1}{2} \int_{\mathcal{V}} [\rho_s + \rho_{\text{ext}}](\mathbf{r}) \phi_{\text{dip}}(z) d\mathbf{r} + \\ & \frac{1}{2} \int_{\mathcal{V}} \rho_{\text{ind}}(\mathbf{r}) [\phi_s + \phi_{\text{ext}}](\mathbf{r}) d\mathbf{r} + \frac{1}{2} \phi_1 (Q_s + Q_{\text{ext}}) \end{aligned} \quad (\text{C.9})$$

and its form differs from Eqn. (C.4) by the term  $\frac{1}{2} \phi_1 (Q_s + Q_{\text{ext}})$ . Before closing this section, we present the expressions for the double counting terms used to evaluate the total energy when the kinetic energy is obtained from the one-electron sum. Note that adding a constant to the K-S potential does not change the kinetic energy and,

therefore,  $\phi_1$  does not need to be included in the K-S potential so the electrostatic part of the double counting term is given by,

$$E_{\text{el,UCP}}^{\text{DC,PC}}(Q_{\text{ext}}) = - \int_{\mathcal{V}} \rho_e(\mathbf{r}) [\phi_s + \phi_{\text{ind}} + \phi_{\text{ext}} + \phi_{\text{dip}}](\mathbf{r}) d\mathbf{r} \quad (\text{C.10})$$

Adding this term to the dipole-corrected, electrostatic potential energy in Eqn.(C.9), one obtains

$$\begin{aligned} [E_{\text{el,UCP}}^{\text{PC}} + E_{\text{el,UCP}}^{\text{DC,PC}}](Q_{\text{ext}}) = & -\frac{1}{2} \int_{\mathcal{V}} \rho_e(\mathbf{r}) \phi_e(\mathbf{r}) d\mathbf{r} + \\ & \frac{1}{2} \int_{\mathcal{V}} \rho_i(\mathbf{r}) \phi_i(\mathbf{r}) d\mathbf{r} + \\ & \frac{1}{2} \int_{\mathcal{V}} [\rho_i - \rho_e(\mathbf{r}) - \rho_{\text{ext}} - \rho_{\text{ind}}](\mathbf{r}) \phi_{\text{dip}}(z) d\mathbf{r} + \\ & \frac{1}{2} \phi_1(Q_s + Q_{\text{ext}}) + \int_{\mathcal{V}} \rho_{\text{ext}}(\mathbf{r}) [\phi_i(\mathbf{r}) + \phi_{\text{dip}}(z)] d\mathbf{r} + \\ & \frac{1}{2} \int_{\mathcal{V}} \rho_{\text{ind}}(\mathbf{r}) [\phi_{\text{ext}} - \phi_e + \phi_i + \phi_{\text{dip}}](\mathbf{r}) d\mathbf{r} \end{aligned} \quad (\text{C.11})$$

Note that in absence of a PC plane  $\rho_{\text{ind}}(\mathbf{r}) = 0$ ,  $Q_s = -Q_{\text{ext}}$  and Eqn. (C.11) reduces to (B.6).

## Appendix D. DFT implementation to include an external, uniformly charged plane

The required computational modifications for the PC model have already been implemented in the VASP code [20] and is described in Ref. [11]. In our new DFT scheme, the inclusion of the repulsive energy and forces over the atoms in the bottom layer of the insulating film is straightforward. The implementation of the DFT method to handle an external, uniformly charged plane UCP,  $\rho_{\text{ext}}(\mathbf{r}) = \sigma_{\text{ext}} \delta(z - z_{\text{ext}})$ , is also rather straightforward. The electrostatic potential  $\phi_{\text{ext}}(\mathbf{r})$  from  $\rho_{\text{ext}}(\mathbf{r})$  is generated in standard manner by solving Poisson's equation in reciprocal space. By adding  $\rho_{\text{ext}}(\mathbf{r})$  to the electronic charge density  $n_s(\mathbf{r})$  allowed us to compute the surface dipole moment that determines the dipole potential through Eqn. (B.3), as well as the dipole energy correction (third term of the RHS of Eqn. (B.6)) using the standard VASP dipole correction subroutine. However, in the case of the PC model with an UCP, the surface dipole moment and the dipole energy correction are computed by adding the  $\rho_{\text{ext}}(\mathbf{r})$  and  $\rho_{\text{ind}}(\mathbf{r})$  to  $n_s(\mathbf{r})$ . Finally, the fifth and sixth terms of the RHS of Eqn. (C.11) have been computed in reciprocal space.

## Appendix E. First order correction for a system interacting with a Perfect Conductor and an external charged plane

Here, we show that the first order correction to the electrostatic energy  $E_{\text{el,UCP}}^{\text{PC}}$  in the PC model to the charge  $Q_{\text{ext}}$  of an external, uniformly charged plane is given by the

difference of the averaged potential of the neutral system between the positions  $z_{\text{ext}}$  and  $z_{\text{PC}}$  of the external plane and the PC plane, respectively. Differentiating the electrostatic energy expression of Eqn. (C.9) with respect to  $Q_{\text{ext}}$ , one obtains,

$$\begin{aligned} \frac{\partial E_{\text{el,UCP}}^{\text{PC}}}{\partial Q_{\text{ext}}}(Q_{\text{ext}}) &= \frac{1}{2A} \int_{\mathcal{V}} \delta(z - z_{\text{ext}}) [2\phi_s(\mathbf{r})d\mathbf{r} + \phi_{\text{dip}}(z)] + \\ &\quad \frac{1}{2A} \int_{\mathcal{V}} \frac{\partial \phi_{\text{dip}}(z)}{\partial Q_{\text{ext}}}(z) [\rho_s + \rho_{\text{ext}}](\mathbf{r})d\mathbf{r} + \frac{1}{2}\phi_1 - \\ &\quad \frac{1}{2A} \int_{\mathcal{V}} \delta(z - z_{\text{PC}}) \phi_s(\mathbf{r})d\mathbf{r} \end{aligned} \quad (\text{E.1})$$

where the dipole potential  $\phi_{\text{dip}}(z)$  is defined in Eqn. (B.3) and the constant  $\phi_1$  is given by Eqn. C.8. Expressing the surface dipole moment  $m$  of Eqn. (C.5) as  $m = m^{(0)} + m^{(1)}$  with  $m^{(0)} = \frac{1}{A} \int_{\mathcal{V}} \rho_s(\mathbf{r})z d\mathbf{r}$  and  $m^{(1)} = \frac{1}{A} \int_{\mathcal{V}} [\rho_{\text{ind}}(\mathbf{r}) + \rho_{\text{ext}}(\mathbf{r})]z d\mathbf{r}$ , and the corresponding contributions  $\phi^{(1)}(z)$  and  $\phi^{(1)}(z)$  to  $\phi_{\text{dip}}(z)$ , one obtains  $\frac{\partial m^{(1)}}{\partial Q_{\text{ext}}} = \frac{(z_{\text{ext}} - z_{\text{PC}})}{A}$  and

$$\frac{\partial \phi_{\text{dip}}}{\partial Q_{\text{ext}}}(z) = \frac{4\pi(z_{\text{ext}} - z_{\text{PC}})}{A} \left[ \frac{z}{L_z} - \frac{1}{2} \right]. \quad (\text{E.2})$$

Inserting  $\frac{\partial \phi_{\text{dip}}}{\partial Q_{\text{ext}}}(z)$  in Eqn. (E.1), one gets after re-arranging terms,

$$\int_{\mathcal{V}} \frac{\partial \phi_{\text{dip}}}{\partial Q_{\text{ext}}}(z) [\rho_s + \rho_{\text{ext}}](\mathbf{r})d\mathbf{r} = [\phi_{\text{dip}}^{(0)}(z_{\text{ext}}) - \phi_{\text{dip}}^{(0)}(z_{\text{PC}}) + \phi_{\text{dip}}^{(1)}(z_{\text{ext}})]. \quad (\text{E.3})$$

and,

$$\begin{aligned} \frac{\partial E_{\text{el,UCP}}^{\text{PC}}}{\partial Q_{\text{ext}}} &= [\bar{\phi}_s + \phi_{\text{dip}}^{(0)}](z_{\text{ext}}) - [\bar{\phi}_s + \phi_{\text{dip}}^{(1)}](z_{\text{PC}}) + \\ &\quad \frac{1}{2} [\phi_{\text{dip}}^{(1)}(z_{\text{ext}}) - \bar{\phi}_{\text{ind}}(z_{\text{PC}}) - \bar{\phi}_{\text{ext}}(z_{\text{PC}})]. \end{aligned} \quad (\text{E.4})$$

Since  $m^{(1)} = 0$  and  $\phi_{\text{dip}}^{(1)} = \phi_{\text{ext}} = 0$  when  $Q_{\text{ext}} = 0$ , and  $\bar{\phi}_{\text{ind}} = 0$  for a neutral system S, we finally obtain the desired result

$$\left. \frac{\partial E_{\text{el,UCP}}^{\text{PC}}}{\partial Q_{\text{ext}}} \right|_{Q_{\text{ext}}=0} = [\bar{\phi}_s + \phi_{\text{dip}}](z_{\text{ext}}) - [\bar{\phi}_s + \phi_{\text{dip}}](z_{\text{PC}}). \quad (\text{E.5})$$

## References

- [1] J. Repp, G. Meyer, S. M. Stojković, A. Gourdon, C. Joachim, Phys. Rev. Lett. **94**, 026803 (2005).
- [2] J. Repp, G. Meyer, S. Paavilainen, F. E. Olsson, M. Persson, Science **312**, 1196 (2006).
- [3] J. Repp, G. Meyer, F. E. Olsson, M. Persson, Science **305**, 493 (2004).
- [4] F. E. Olsson, S. Paavilainen, M. Persson, J. Repp, G. Meyer, Phys. Rev. Lett. **98**, 176803 (2007).
- [5] F. Mohn, J. Repp, L. Gross, G. Meyer, M. S. Dyer, M. Persson, Phys. Rev. Letter **105**, 266102 (2010).
- [6] L. Gross, F. Mohn, P. Liljeroth, J. Repp, F. J. Giessibl, G. Meyer, Science **324**, 1428, (2009).
- [7] J. Repp, P. Liljeroth, G. Meyer, Nature Physics **6**, 975 (2010).
- [8] P. Liljeroth, J. Repp, G. Meyer, Science **317**, 1203 (2007)
- [9] Cohen A.J., Mori-Sanchez P. and Yang W., Science, **321** (5890): 792-794 (2008)
- [10] B. Kaduk, T. Kowalczyk, T. Van Voorhis, Chemical Reviews **112**, 321 (2012).
- [11] I. Scivetti and M. Persson, Journal of Physics: Condensed Matter **25**, 355006 (2013).

- [12] P. Hohenberg and W. Kohn, Phys. Rev., **136**, B-864, (1964).
- [13] W. Kohn and L. J. Sham, Phys. Rev., **140**, 1133A, (1965).
- [14] V. I. Anisimov, J. Zaanen, and O. K. Andersen, Phys. Rev. B **44**, 943 (1991); V. I. Anisimov, I. V. Solovyev, M. A. Korotin, M. T. Czyzyk, and G. A. Sawatzky, *ibid.* **48**, 16929 (1993).
- [15] M. Cococcioni, S. de Gironcoli, Phys. Rev. B **71**, 035105 (2005).
- [16] A. S. Martins, A. T. da Costa, P. Venezuela, R. B. Muniz, Eur. Phys. J. B **78**, 543 (2010).
- [17] N. D. Lang and W. Kohn, Phys. Rev. B **1**, 4555 (1970)
- [18] N. D. Lang and W. Kohn, Phys. Rev. B **3**, 1215 (1971)
- [19] N. D. Lang and W. Kohn, Phys. Rev. B **7**, 3541 (1973)
- [20] G. Kresse, J. Furthmuller, Phys. Rev. B **54**, 11169 (1996); G. Kresse, D. Joubert, Phys. Rev. B **59**, 1758 (1999).
- [21] Blöch P.E. , Phys. Rev. B **50**, 17953-17979, (1994).
- [22] W. Chen, C. Tegenkamp, H. Pfnur, and T. Bredow, Phys. Chem. Chem. Phys., **11**, 9337 (2009)
- [23] J. Björk, F. Hanke, C.-A. Palma, P. Samori, M. Cecchini, and M. Persson, The Journal of Physical Chemistry Letters, 1, 3407 (2010), <http://pubs.acs.org/doi/pdf/10.1021/jz101360k>
- [24] J. Klimeš D. R. Bowler, and A. Michaelides, Journal of Physics: Condensed Matter, **22**, 022201 (2010)
- [25] J. Klimeš D. R. Bowler, and A. Michaelides, Phys. Rev. B, **83**, 195131 (2011)
- [26] The super cell dimensions are  $L_x=L_y=7.638 \text{ \AA}$  and  $L_z=31.20 \text{ \AA}$
- [27] J. Repp, G. Meyer, S. M. Stojković, A. Gourdon, C. Joachim, Phys. Rev. Lett. **94**, 026803 (2005).
- [28] J. P. Perdew, K. Burke, and M. Ernzerhof, Phys. Rev. Lett. **77**, 3865 (1996).
- [29] J. Neugebauer and M. Scheffler, Phys. Rev. B **46**, 16067 (1992).
- [30] L. Bengtsson, Phys. Rev. B **59**, 12301 (1999).
- [31] Martin, R. M., *Electronic Structure: Basic Theory and Practical Methods*, (Cambridge, UK, 2004).
- [32] If the external plane is sufficiently far from the surface, the value of  $\Phi$  will be equal to the work function of the system.
- [33] I. Scivetti and M. Persson (in preparation).